THE EFFECT OF DC VOLTAGE ON FIBROUS DEBRIS BYPASS THROUGH A CONTAINMENT SUMP STRAINER

A Thesis

by

TODD ANDREW WILLIAMS

Submitted to the Office of Graduate and Professional Studies of
Texas A&M University
in partial fulfillment of the requirements for the degree of

MASTER OF SCIENCE

Chair of Committee,	Yassin A. Hassan
Committee Members,	William H. Marlow
	Maria D. King
	Victor M. Ugaz
Head of Department,	Yassin A. Hassan

December 2016

Major Subject: Nuclear Engineering

Copyright 2016 Todd Andrew Williams

ABSTRACT

Public safety has long been one of the chief design concerns for Nuclear Power Plants (NPPs). For this reason, the design of a NPP must include plans for different accident scenarios called Design Basis Accidents (DBAs). One such DBA is called a Loss of Coolant Accident (LOCA); Pressurized Water Reactors (PWRs) are particularly prone to them.

In order to better understand the phenomena associated with a LOCA, a great deal of research has been undertaken. In particular, many studies have been done under the designation Generic Safety Issue-191 (GSI-191). GSI-191 seeks to better understand the secondary effects of a LOCA such as the pressure drop and debris bypass of the containment sump strainer and the impact that both can have on the Emergency Core Cooling System (ECCS).

The present study was undertaken to build upon previous work that sought to determine whether or not a voltage applied to the sump strainer would affect the amount of fibrous debris bypass. To this end, a vertical strainer made from a perforated steel plate was installed in a horizontal flow loop. A filter bag was installed downstream from the strainer to collect the debris bypass. The fibrous debris was made from one-side baked NUKON fiberglass insulation. Measurements were also taken of the pressure drop across the debris beds. A total of 19 tests were carried out across five different voltages.

No significant difference was observed in either the bypass or the pressure drop between the different voltages. The test results may have been affected by the fact that the present study involved water that was cooler than previous studies. The results may have also been affected by leaks in the test section. Furthermore, the use of multiple NUKON

mats may also have affected the results. A study on the sensitivity of the debris bypass to kinematic viscosity could help shed some light on the former problem.

ACKNOWLEDGMENTS

First and foremost, I would like to thank my loving wife for all the support that she has given me throughout my collegiate endeavors. I would also like to thank my two daughters, Adeline and Ruby for cheering me up when things have been bleak.

Additionally, I would like to thank those in the department who have helped me get to this point, namely, Dr. Yassin Hassan, Dr. Rodolfo Vaghetto, and Dr. Saya Lee.

NOMENCLATURE

ANOVA	Analysis of Variance
DBA	Design Basis Accidents
DC	Direct Current
DI	Deionized
DSLR	Digital Single Lense Reflex
EC	Electrical Conductivity
ECCS	Emergency Core Cooling System
GSI	Generic Safety Issue
ID	Inner Diameter
LOCA	Loss of Coolant Accident
NEI	Nuclear Energy Institute
NPP	Nulcear Power Plant
NPSH	Net Postive Suction Head
STP	South Texas Project

TABLE OF CONTENTS

Page

LIST OF FIGURES

FIGURE Page

LIST OF TABLES

TABLE Page

1. INTRODUCTION

Solid-liquid filtering has many applications in a number of fields. Historically speaking, filtration was likely first used as a means of water treatment [1]. Additionally, filtration has applications in chemical processing [2], as well as the food and beverage industry [3]. Solid-liquid filtration is also of interest to NPPs, especially in the ECCSs of PWRs.

NPPs make extensive use of fibrous insulation materials. While these materials provide excellent insulation and can protect plant components from adverse thermal effects, they have shown potential to cause failure of the ECCS during a LOCA. Extensive research in this field has been done under the designation, Generic Safety Issue (GSI) 191, Assessment of Debris Accumulation on PWR Sump Performance, [4]. During such an event, coolant is lost due to a pipe break. The resulting high velocity jet can dislodge thermal insulation materials and break structural components. Some of the resulting debris can be transported to the containment sump strainer where it can cause a loss of Net Positive Suction Head (NPSH) [5]. Additionally, some of the debris can be transported through the strainer where it may become lodged in any of the components downstream of the strainer [6]. Debris transport to, and buildup on the sump strainer falls under the category of upstream effects. Debris bypass of the strainer and the negative effects that stem therefrom are categorized as in vessel effects.

2. LITERATURE REVIEW

Much research has been done to better understand the phenomena involved in GSI-191 events. Studies on the upstream effects have examined what factors affect the amount of debris that is transported to the strainer [7], the buildup of a debris bed over time [8-10], and the pressure drop that such debris beds cause [8, 10, 11].

Studies of the in-vessel effects focus primarily on identifying parameters that affect the amount of debris that makes it through the sump strainer, or in other words, parameters that affect the efficiency of the filtration provided by the strainer. In order to identify variables that could potentially affect filtration, it is necessary to understand filtration phenomena. Hutten identifies four different filtration mechanisms [12]. Of Huttens four types of filtration, depth filtration is often believed to be the mechanism primarily responsible for preventing debris bypass of the sump strainer [13].

Studies on depth filtration done by researchers outside the field of nuclear engineering have identified a number of factors that influence the efficiency of depth filtration, including pH [14, 15] and ionic strength [15]. It is theorized that these factors change the filtration efficiency by changing the double layer repulsion forces [16].

Many studies were undertaken to prove that the same principles held true for the conditions that exist during a LOCA [13, 17-19]. These studies have shown that there is a positive correlation between pH and the amount of debris bypass, while Electrical Conductivity (EC) above a certain threshold (840 μS/cm) reduces the amount of debris bypass.

Recognizing that electric potential affects double layer repulsion energy [20], Lee et al. hypothesized that a voltage applied to the sump strainer would have significant impact on the amount of debris bypass [13]. While their research showed promise, only single

tests were run for each of the voltages tested. Additional tests must be run in order to assess the statistical significance of the results.

3. RESEARCH OBJECTIVE AND APPROACH

The objective of this study is to build upon the work by Lee et al. [13] with regards to bypass tests with a voltage applied to the strainer. More specifically, the goal is to run replicates of the previous experiments so that a conclusion can be reached concerning the effect of voltage on debris bypass.

The same horizontal flow loop utilized by Lee et al. will be used for the present study. A rendering of the facility can be seen in Figure 1. There are a number of key features to the test facility. First, there is the water tank, where prepared debris is poured to initiate the test. A mixing propeller is installed in the tank so as to try and keep the debris concentration as uniform as possible throughout the tank. Submerged in the tank, there is a wire connected to one of the terminals of a DC voltage controller.

The test section contains three key components, a pressure transducer, the strainer, and the filter bag. Although not pertinent to the present study, head loss through the debris bed is measured by the pressure transducer and recorded (should future researchers require the information for their own purposes). The strainer was manufactured so as to be representative of a PWR sump strainer and is connected by a wire to the other terminal of the DC voltage controller. A filter bag is installed to capture any debris that passes through the debris bed and strainer. The flow rate is controlled through the use of a pump operated with a variable frequency drive as well as a control valve. An electromagnetic flow meter is used to measure the flow rate.

4. EXPERIMENTAL FACILITY AND CONDITIONS

4.1 Experimental Conditions

The experimental conditions for the present study were set to be identical to the previous work by Lee et al. [13] as summarized in Table 4.1. The area averaged approach velocity was set to 0.12 in/s (0.3 cm/s). This flow rate was selected based on the surface area of the South Texas Project (STP) sump strainer of 1818.5 ft^2 (168.9 m^2) and a nominal flow rate of 7020 gal/min (26.6 m^3/min) [20].

Each test is run with 0.23 oz, (6.6 g) of NUKON debris. Given that the facility is filled with 51.5 gallons (195 L) of water, the initial NUKON concentration is 0.0034% by weight and 0.09% by volume.

All tests were run with local tap water at room temperature. The EC of the water used was 768.2$\pm$179.6 μS/cm. The pH was found to be 8.16$\pm$0.48. Additionally, the water temperature was found to be 69.8 $\pm$ 4.7°F (20.96 $\pm$ 2.6°C).

Four different voltages were applied to the strainer. Two positive voltages of +1 V and +0.5 V were used, in addition to two negative voltages, -1 V and -0.5 V.

Table 4.1: Target experimental conditions.

Target/Expected Parameter Values	
Tempurature	25±3°C
Approach Velocity	0.3 cm/s
Initial debris mass	6.6 g
pH	8.56
Electrical conductivity	840 µS/cm

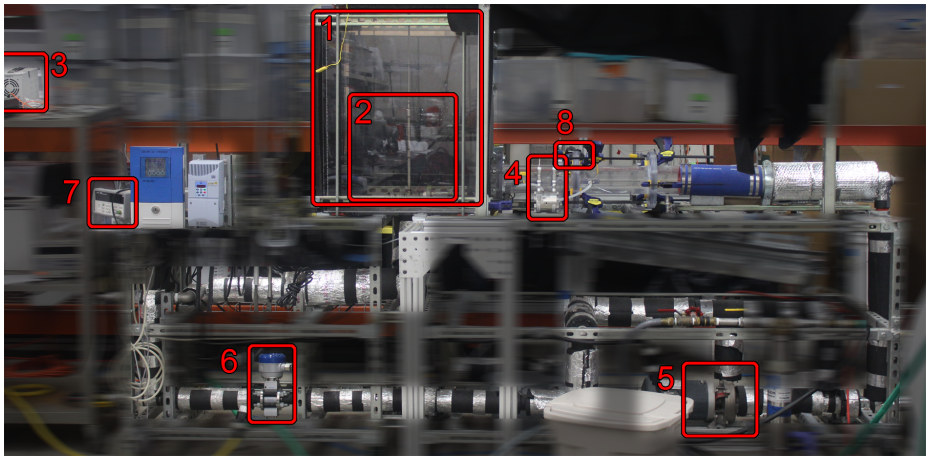

Figure 4.1: Experimental facility (with key components emphasized and numbered).

Each test is run for a total of 2 hr and 5 min. This time was calculated based on one turnover of the system.

4.2 Experimental Facility

The facility can be seen in Figure 4.1 and important components are listed in Table 4.2.

Table 4.2: Major components of the experimental facility.

Item Number	Item
1	Water tank
2	Mixing propeller
3	Korad KA 3010D power supply
4	Honeywell differential pressure transducer model The
5	MP Pumps ChemFlow® Series
6	Krohne Opitflex 1000 F electromagnetic flow meter
7	Agilent Technologies 4972A LXI Data Acquisition/Data Logger Switch Unit
8	Nikon D7000 DSLR

4.2.1 Water Tank

The tank is made from transparent polycarbonate. The base of the tank measures approximately 24" × 24" (60.96 cm × 60.96 cm) with walls approximately 30" (70.2 cm) high. Key heights are marked on the outside of the tank. The top is open to the air for filling the facility with water and for injecting the debris. In the middle of the base is the return pipe measuring 1" (2.54 cm) Inner Diameter (ID). On the side of the tank is the outlet pipe which measures 4" (10.16 cm) ID. The outlet pipe leads immediately into the test section.

4.2.2 Mixing Propeller

The mixing propeller, which can be seen in Figure 4.2, was manufactured in house from steel bars and pipes. It hangs in the tank directly above the return pipe. It's function is to stir the water in the tank to try and keep the debris concentration as uniform as possible. The motor is connected to a time delay relay (see Figure 4.3) which is set to reverse the direction of rotation every minute [22]. This is done to prevent the buildup of debris on the mixing propeller [8].

4.2.3 DC Power Source

The DC voltage is applied to the strainer and the water tank through the use of a Korad KA3010D power supply. The device has maximum outputs of 30 V and 10 A. Additionally, the voltage can be set in 10 mV increments and the current in increments of 1 mA [23].

4.2.4 Strainer

The strainer, which can be seen in Figure 4.5, is designed to be representative of the containment sump strainer used by the STP [20]. It is made from stainless steel and is

Figure 4.2: Mixing propeller.

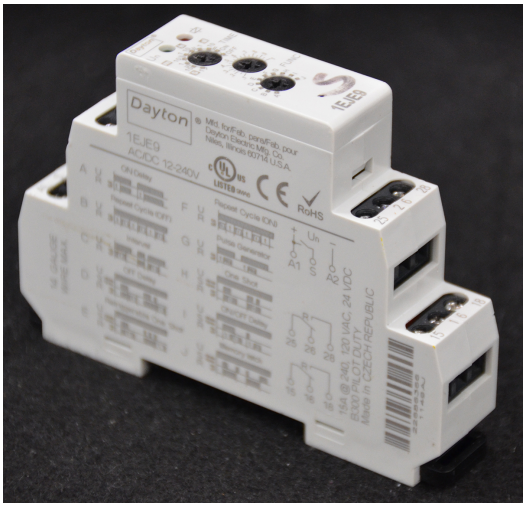

Figure 4.3: Dayton® Time Delay Realy Model# 1EJE9 (used to control mixing propeller direction).

Figure 4.4: DC power supply (Korad KA3010D).

0.06” (1.56 mm) thick. Holes in the strainer have a diameter of 0.095” (2.42 mm) and have a lattice pitch of 0.16” (3.96 mm).

4.2.5 Pressure Transducer

The pressure drop across the test section is measured with a Honeywell differential pressure transducer model TJE (see Figure 4.6). This model supports measurements up to 1 psid with a resolution of 0.001 psid [24]. It is connected to the sides of the test section by means of two flexible tubes, one connected upstream of the strainer and the other downstream. The upstream tube is attached approximately 10” (25.4 cm) away from the strainer. This is done to allow for head loss tests to also be performed at the same facility. Past tests have shown that debris beds in such tests can be as much as 9” (22.86 cm) or more. The other tube is connected in between the strainer and the filter bag.

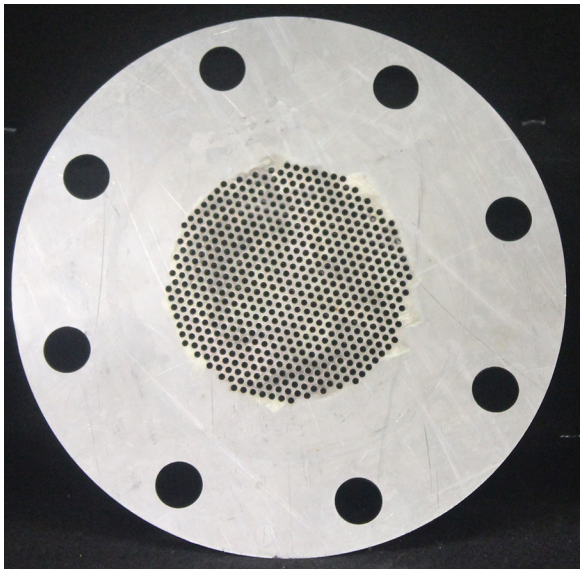

Figure 4.5: Stainless steel strainer.

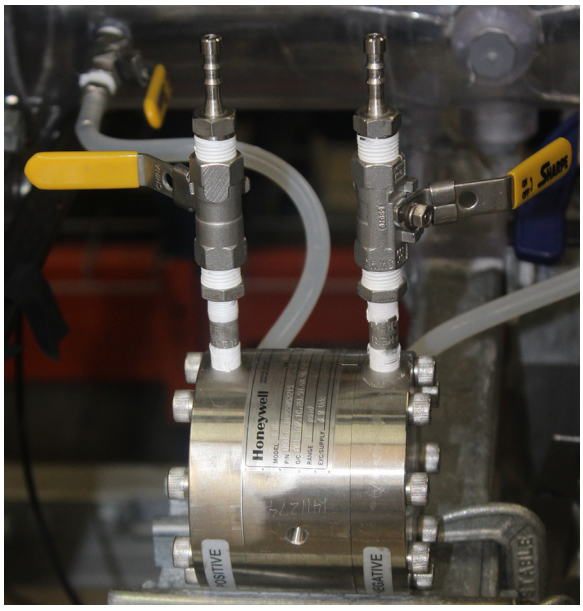

Figure 4.6: Differential pressure transducer (Honeywell Model TJE).

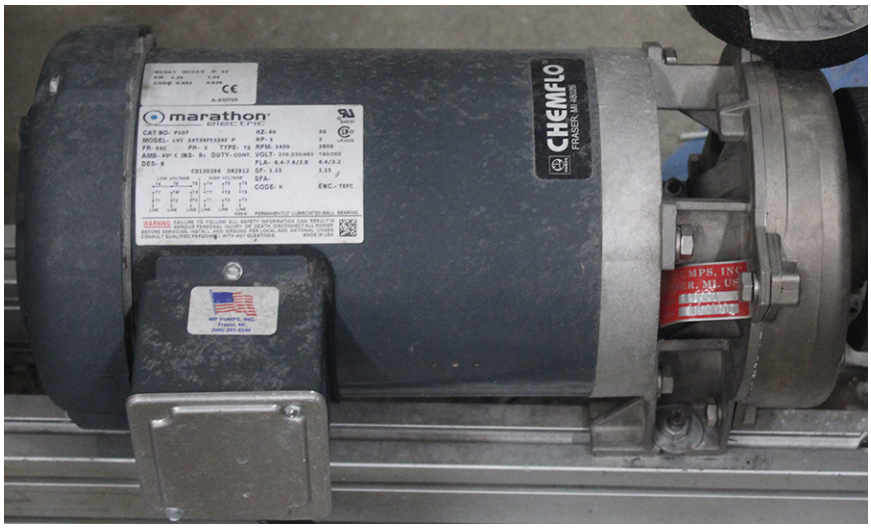

Figure 4.7: MP Pumps ChemFlow® pump (with attached Marathon Electric motor).

4.2.6 Pump

The circulation pump is a MP Pumps ChemFlow® Series that is driven by a Marathon Electric Model LV3 electric motor (see Figure 4.7). The speed of the motor is controlled though the use of WEG Variable Speed Drive CFW08 (see Figure 4.8).

4.2.7 Flow Meter

The flow is measured by a Krohne Optiflex 1000 F electromagnetic flow meter (see Figure 4.9). This model has an accuracy of 0.5% of the measured value for flow rates above about 1.64 ft/s (0.5 m/s), but accuracy is reduced to approximately 1.1% below this speed. It is designed so that it can be safely operated with fluid temperatures varying from -13 and +248°F (-25 and +120°C) and an ambient temperature range of -13 and +149°F (-25 and 65°C). Pressure drop through the device is reportedly negligible.

The flow meter operates based on Faraday's Law of Induction [25]. When a conductive fluid flows through an electrically insulated pipe in which a magnetic field is present, a voltage is induced in the fluid according to

Figure 4.8: Variable frequency driver (WEG Variable Speed Drive CFW08).

$$U = v\ k\ B\ D \tag{4.1}$$

where U is the induced voltage, v is the average flow velocity, k is a factor that corrects for geometry, B is the magnetic field strength, and D is the inner diameter of the flow meter [25].

4.2.8 Data Acquisition

Data from the flow meter, thermocouple, and pressure transducer are recorded and saved to a computer through the use of an Agilent Technologies 34972A LXI Data Acquisition/Data Logger Switch Unit. The unit comes bundled with BenchLink data logger software for configuring the data acquisition. It can read 11 different types of signals including thermocouple signals, thermisters, and DC/AC voltage and current [26].

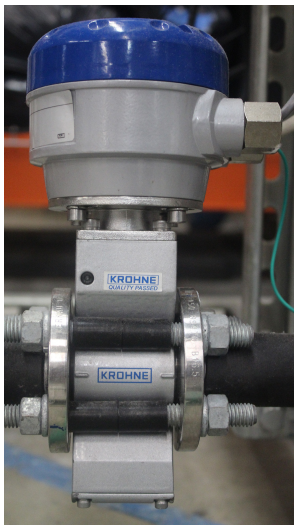

Figure 4.9: Krohne Optiflex 1000 F electromagnetic flowmeter.

4.2.9 Camera

A Nikon D7000 Digital Single Lens Reflex (DSLR) is used to photograph the test section while the test is running (see Figure 4.11). The camera can capture images in up to 16.2 mega-pixels and can be set to take up to 999 pictures at rates up to 1 Hz.

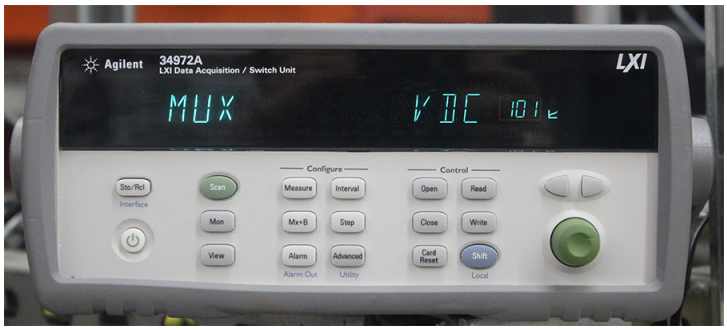

Figure 4.10: Data acquisition device (Agilent Technologies 34972A LXI Data Acquisition/Data Logger Switch Unit).

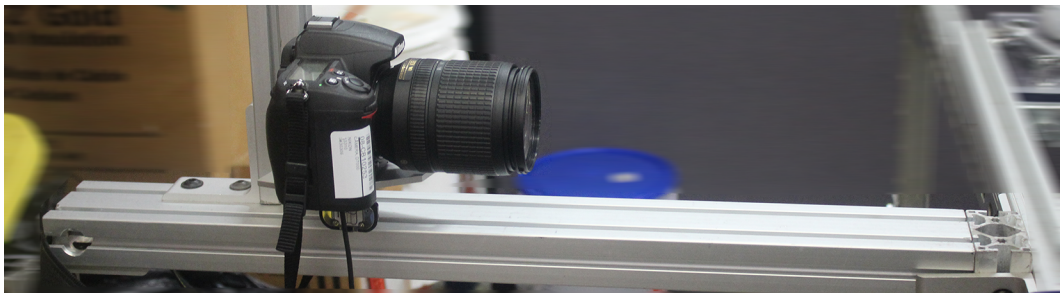

Figure 4.11: Nikon D7000 DSLR (mounted on its stand).

4.2.10 pH Meter

The pH of the water was measured using a Mettler Toledo SevenCompact^{TM} S220 pH/ion meter. The meter can measure pH values between -2.000 and 20.000 with a resolution of up to 0.001. Additionally, the manufacturer states that it is accurate to within $\pm$0.002 [28].

Figure 4.12: pH meter (Mettler Toledo SevenCompact^{TM} S220 pH/ion meter).

Figure 4.13: Electrical conductivity meter (PCSTestr^{TM} 35).

4.2.11 EC Meter

The EC of the tap water is measured using an OAKTON® PCSTestr^{TM} 35 manufactured by Eutech Instruments (see Figure 4.13). This hand handheld meter is able to read EC, pH, TDS, salinity, and temperature. It is equipped with automatic calibration. This means that for measured values in a given range, the device will assume a standard calibration value (see Table 4.3).

Measured Value Range	Automatic Calibration Value
0.0 - 200.0 µS/cm	84 µS/cm
200.0 - 2000 µS/cm	1413 µS/cm
2.01 - 20.00 mS/cm	12.88 mS/cm

Table 4.3: PCSTestr^{TM} 35 automatic calibration data.

5. TEST PROCEDURE

Procedures for running the test are perhaps best broken up into three parts, pretest, test, and post-test. Pretest procedures include everything that can, if needed, be performed the day before the test is actually run. Test procedures include the test itself and everything that typically must be done on the same day as the test. Lastly, the post-test procedures involves everything that either can, or must be done the day after the test is run.

5.1 Pre-Test Procedures

The pre-test phase involves four parts, instrument calibration, cleaning, filter preparation, and debris preparation.

Three instruments, the flow meter, thermocouple, and pressure transducer, must be calibrated before a test. The flow meter is calibrated by adjusting the valves so that the water does not circulate, but rather drains out and into a graduated cylinder. The system is drained in this manner for a predetermined amount of time (depending on the flow rate), the flow rate is then calculated and compared to the signal from the flow meter. The thermocouple is calibrated by heating water on a hotplate to different target temperatures and comparing the recorded temperature to the value measured by a digital thermometer whose accuracy is guaranteed by the manufacturer. Finally, the pressure calibration is verified by applying pressure to both the transducer and a manometer using a syringe.

The pretest cleaning procedures calls for an unused filter to be placed in the outlet of the tank, the tap water line to be placed in the tank, and the valves to be set such that water drains from the facility, rather than circulating through it. After each test, more thorough cleaning procedures are performed. The post-test cleaning consists of three phases. The first phase is identical to the pretest procedure. In the second phase, the tap water line is shut off, and the valves are adjusted so that water continuously circulates through the

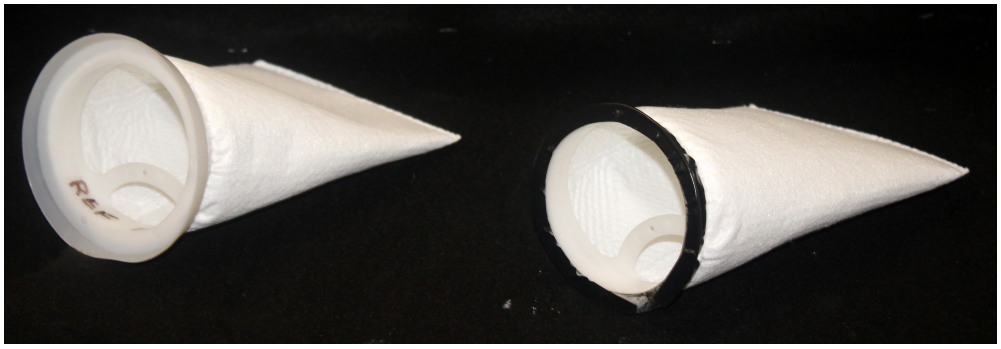

Figure 5.1: Filter preparation (filter as it arrives from the manufacturer is seen left and a filter cut to fit in the test section is seen right).

facility, rather than draining out. The third phase is similar to the first, but the filter is removed from the tank outlet.

The filters used in this study are made from 1 μm heat-welded felt and come with a plastic ring head. First, the ring heads must be trimmed in order for the filter to properly fit in the test section (see Figure 5.1). In order to account for the water content in the filter due to ambient humidity, a reference filter is weighted along with the test filter. The two filters are set side by side for an hour, after which the weight of each filter, along with the ambient temperature, and the ambient humidity are all recorded.

The last thing that must be completed as part of the pretest phase is the preparation of the debris to be used. The preparation procedures are based on the Nuclear Energy Institute (NEI) fine debris preparation procedure [21]. From a mat of one-side baked NUKON (see Figure 5.2), an initial block measuring approximately 2" $\times$ 2" (5 cm $\times$ 5 cm) is cut as seen in Figure 5.3.

The block of NUKON is trimmed as necessary in order to achieve a weight of 0.23 oz (6.6 g). Once the desired amount of NUKON has been measured out, it is placed in a bucket (see Figure 5.4). The NUKON block is then broken up in three steps (see Figure

Figure 5.2: Typical NUKON mat.

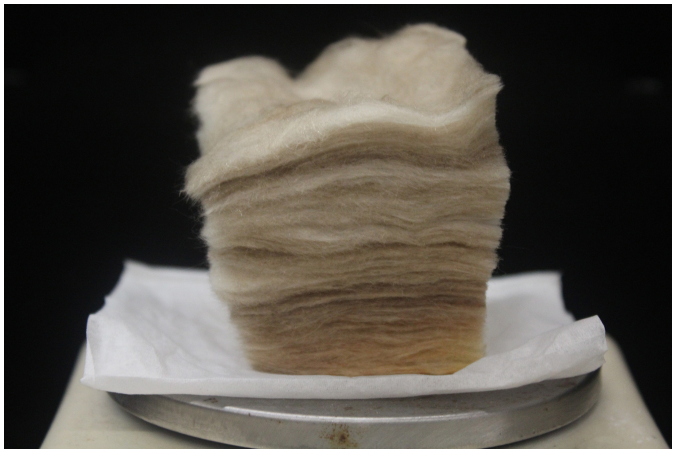

Figure 5.3: Initial NUKON block.

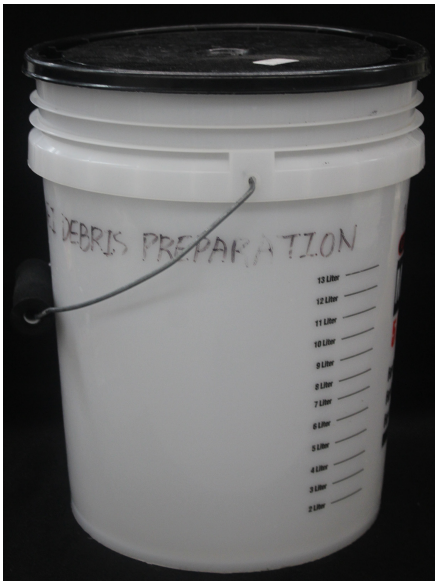

Figure 5.4: NUKON debris preparation bucket.

5.5). First, the block is cut into four pieces, the burnt layers of each piece are separated from the clean layers, lastly the charred layers are then separated into fourths with the clean layers separated into eights. The bucket is then filled with water in two steps (see Figure 5.6). First, the bucket is filled to the 0.5 gallon (1.89 L) mark using a high pressure power washer (see Figure 5.7), a 40° nozzle is then fitted to the power washer, the lid is placed on the bucket, the nozzle is inserted through a hole in the top of the bucket, and the power washer is used to fill the bucket to the 5 gallon (18.93 L) mark.

The filter and NUKON having been prepared, the test facility must next be readied for a test. After ensuring that the cleaning procedures have been completed and the facility is empty, the tank is filled to the 8" (20.32 cm) mark with tap water and, while the water is still running, the valves are adjusted so that the water flows out through the drain, and the circulation pump is turned on. After 15 minutes, the water and the pump are switched off and the tank is allowed to drain. The tank is then filled to the same mark and drained

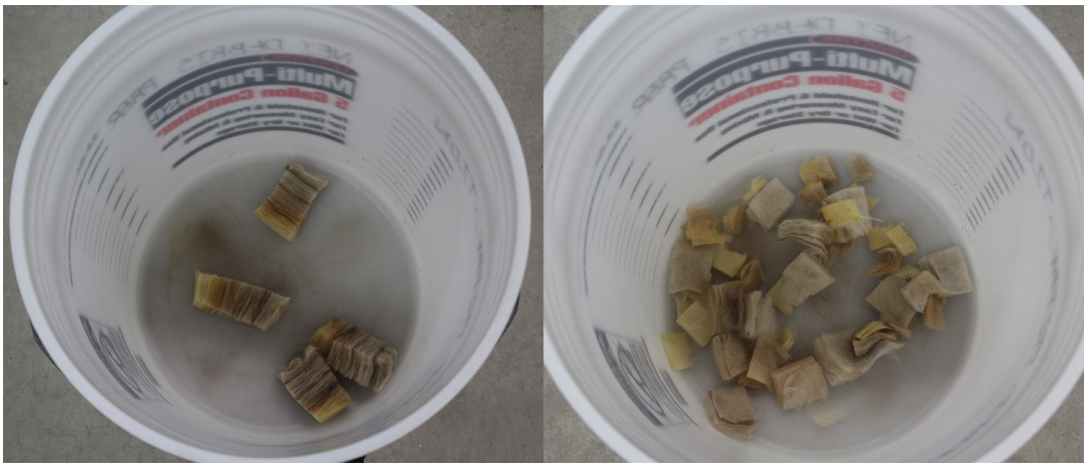

Figure 5.5: NUKON separation process (NUKON after being cut into four pieces is seen left and after the layers have been separated according to test procedures is seen right).

Figure 5.6: Nukon bucket filling process (the 0.5 gallon mark is seen left and the 5 gallon mark is seen right).

Figure 5.7: High pressure washer.

immediately. Next, the test section is removed and the filter is inserted into the pipe, using a silicone gasket to hold it in place (see Figure 5.8). The test section is then bolted back into place. With the filter in place, the tank is filled to the 19" (48.26 cm) mark and the flow rate is set by adjusting the circulation pump and a ball valve located downstream from the pump.

The instruments are checked one last time. The focus and zoom on the camera are adjusted as needed to ensure that clear pictures will be taken of the test section. The camera is also set to take pictures in 8s intervals. The data acquisition system is activated to ensure that the flow meter, thermocouple, and pressure transducer are all operating normally and the data is being properly recorded. The power source must then be connected to the system. A wire from one end is taped externally to the strainer while the other end is attached to a small pipe that is partially submerged in the tank. The test is then ready to begin.

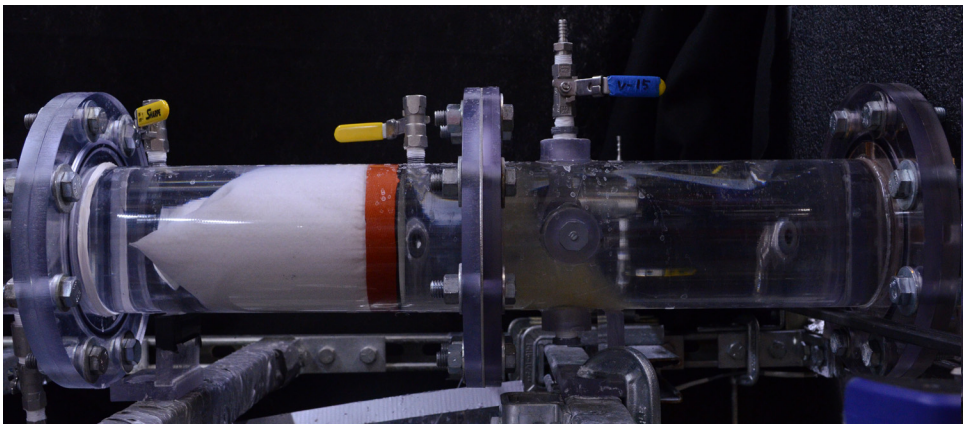

Figure 5.8: Silicone gasket (seen here holding the test filter in place).

5.2 Test Operation Procedures

To begin the test, five actions must be completed. First, the power source and mixing propeller must be activated. Next, the camera must be started, the NUKON must be poured quickly over ≈5s in the tank, and the data acquisition must be started. Following this, a small sample (≈ 0.68 fl oz or 20 mL) is taken from the tank so that the EC and pH can be measured. Before this can be done, both instruments are calibrated. The EC meter is calibrated using solutions of 84 and 1413 μS/cm while solutions of 4.01, 7.01 and 10.01 are used for the pH meter. The sample is returned to the tank after being measured. Additional samples are taken and measured at the 1 hour and 2 hour marks. The test is then terminated after 2 hours and 5 min.

5.3 Post Test Procedures

When the timer indicates the test has finished, the mixing propeller and pump are turned off. A plug is inserted into the tank outlet, and a valve located approximately 6.5' (2m) downstream from the strainer is closed. This is done to isolate the test section from

the rest of the facility. Three valves at the top of the test section are opened along with a valve at the bottom to allow the test section to drain completely.

After the test section is drained, the test section is unbolted and removed. Because of the presence of some debris that has bypassed the strainer, but settled before reaching the filter bag, the test section is lightly rinsed with deionized (DI) water. After all debris in the test section has been collected in the filter, it is removed from the test section. DI water is then used to rinse the filter bag itself. This is done to remove any impurities that may have soaked into the filter bag from the tap water. After being rinsed, the filter bag is hung to dry for 15 minutes to remove excess water before being wrapped in paper towels and set on a warm surface to dry for at least 15 hours. After the filter has dried, it is weighed using the same procedure specified in section 5.1. The bypass mass is then calculated using

$$m_b \;=\; m_{t2} - m_{t1} - (m_{r2} - m_{r1}) \tag{5.1}$$

where m_b is the mass of the bypass, m_{t1} and m_{t2} are the masses of the test filter before and after the test respectively, and m_{r1} and m_{r2} are the masses of the reference filter before and after the test respectively.

6. RESULTS AND DISCUSSION

A plot of the bypass results from the present and previous studies can be seen in Figure 6.1. A plot of the head loss over time can be seen in Table 6.2. When the pattern observed by Lee et al was not seen in the present study, additional tests were run at an increased voltage level (-2 V) in hopes that a pattern would emerge. Additional parameters measured during the experiments can be found in Table 6.1. It should be noted that, with pH values of 8.16 $\pm$ 0.48 and EC at 786 $\pm$ 89 μS/cm, both parameters were within ranges such that their effect on the bypass would have been negligible.

Additionally, it should be noted that the results appear to vary in two different ways from past experiments. First, the mean bypass value in the present study was higher than previous bypass studies. For the present study, the mean was found to be 0.60 $\pm$ 0.09 g while tests run at the same approach velocity, with tap water, but without any applied voltage had a mean of 0.46 $\pm$ 0.02 g [17].

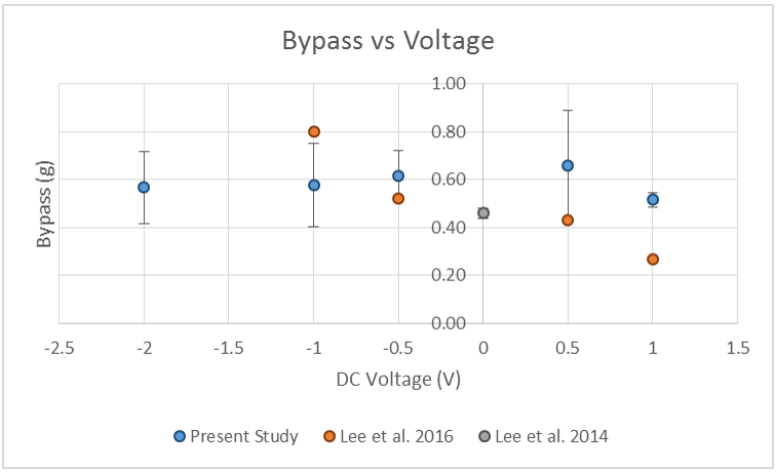

Figure 6.1: Bypass test results.

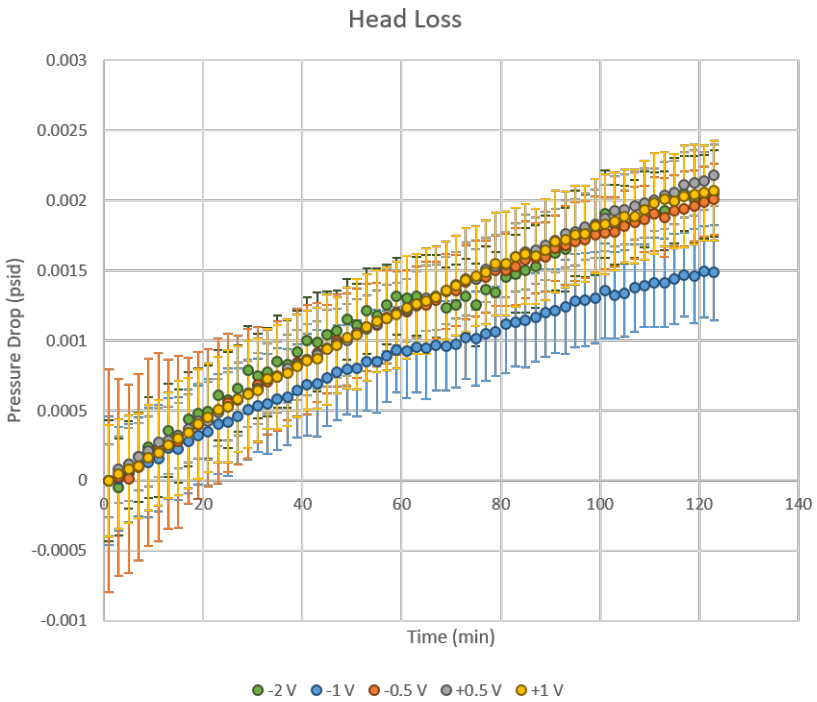

Figure 6.2: Head loss over time.

Voltage (V)	pH	EC (µS/cm)	Flow (in/s)	Temp (°C)	Bypass (g)
-2	7.93	833	0.1188	21.19	0.51
-2	8.42	900	0.1180	21.33	0.65
-2	8.74	873	0.1177	21.02	0.54
-1	7.94	783	0.1172	23.79	0.63
-1	8.13	775	0.1178	23.83	0.45
-1	8.02	764	0.1176	22.17	0.58
-1	8.48	791	0.1178	19.71	0.65
-0.5	8.00	758	0.1184	21.55	0.57
-0.5	7.70	640	0.1176	20.90	0.68
-0.5	8.10	738	0.1180	21.30	0.64
-0.5	8.12	880	0.1184	19.89	0.58
0.5	8.36	713	0.1176	20.23	0.58
0.5	8.14	693	0.1183	19.33	0.53
0.5	8.07	598	0.1184	20.37	0.65
0.5	8.11	792	0.1188	20.06	0.83
0.5	8.28	774	0.1176	20.43	0.70
1	8.31	860	0.1180	19.83	0.51
1	7.94	594	0.1176	21.97	0.50
1	8.26	837	0.1180	19.34	0.53
Average	8.16	768.2	0.118	20.96	0.60
Standard Deviation	0.24	89.8	0.00044	1.30	0.09

Table 6.1: Test results.

7. ANALYSIS

In order to determine with statistical certainty whether or not the different voltages affect the bypass, a single factor Analysis of Variance (ANOVA) was performed. The process of conducting an ANOVA is described in Section 7.1.

7.1 ANOVA

The first step in an ANOVA is to calculate the mean value for each treatment level using

$$\overline{Y}_j = \frac{1}{n_j}\sum_{i=1}^{n_j} Y_{ji} \tag{7.1}$$

where $\overline{Y}_j$ is the arithmetic mean of the of the j^{th} treatment level, n_j is the number of measurements in the j^{th} treatment level, and Y_{ji} is the value of the i^{th} measurement in the j^{th} treatment level. The overall mean can then be calculated from the individual means

$$\overline{Y} = \frac{1}{m}\sum_{j=1}^{m} \overline{Y_j} \tag{7.2}$$

where $\overline{Y}$ is the overall mean of all measurements and m is the number of treatments.

Having calculated the necessary means, the so called between-group sum of squared differences, S_B can be calculated using

$$S_B = \sum_{j=1}^{m} n_j(\overline{Y}_j - \overline{Y})^2 \tag{7.3}$$

The between-group sum of squared differences is then used in conjunction with the degrees of freedom, f_b, which is calculated using

$$f_b \;=\; m - 1 \tag{7.4}$$

to calculate the between group mean square value using

$$MS_B \;=\; \frac{S_B}{f_b} \tag{7.5}$$

where MS_B is the between group mean square value.

The final step is to calculate so called within-group parameters. First there is the within group sum of squares which is calculated using

$$S_w \;=\; \sum_{j=1}^{m} \left(\sum_{i=1}^{n} (\overline{Y}_j - Y_{ji})^2 \right) \tag{7.6}$$

where S_w is the within-group sum of squares. The within group degrees of freedom is then calculated using

$$f_w \;=\; a(n-1) \tag{7.7}$$

where f_w is the within-group degrees of freedom and a and the total number of elements across all treatments. The within-group mean square value is then calculated using

$$MS_w \;=\; \frac{S_w}{f_w} \tag{7.8}$$

where MS_w is the within-group mean square value. Finally, the F-ratio is calculated using

$$F \;=\; \frac{MS_B}{MS_w} \tag{7.9}$$

where F is the F-ratio.

Single factor ANOVA for the bypass data yields an F-ratio of 1.57. At the 5% confidence level, the critical value for F is 3.11. The calculated value being below the critical value indicates that the observed differences in the different voltages can be explained by random variation in the data.

Furthermore an ANOVA was performed on the head loss values recorded at the end of the tests. Doing so resulted in a P-value of 0.235, which means that, while the tests at +1 V demonstrate lower pressure drop, it is not lower by a statistically significant amount. Additionally, this implies that the voltage does not affect the pressure drop or, by extension, the debris bed formation.

7.2 Bypass

Having been unable to substantiate the hypothesis that different voltages produce different outcomes on the bypass, all further analyses will be performed on the supposition that all the test results from the present study constitute a single sample. With that in mind, the next phase was to investigate the abnormally high mean and standard deviation of the bypass in the present study. To this end, an F-test was performed using the data from the present study compared to the study by Lee et al. where the conditions were identical, save it be that no voltage was applied to the strainer [17].

An F-test is performed as follows. The mean values for each sample are calculated using equation 7.1. The variance of each sample is calculated using

$$S_j^2 = \frac{1}{k_j - 1} \sum_{i=1}^{k_j} (\overline{Y_j} - Y_i)^2 \tag{7.10}$$

where S_j is the variance of the j^{th} sample, k_j is the number of elements in the j^{th} sample, and Y_i is the value of the i^{th} element. The F-ratio is then calculated using

$$F = \frac{S_1^2}{S_2^2} \tag{7.11}$$

In comparing the present study to previous [17], the F-test resulted in a P-value of 0.032, meaning that the differences between the two samples is statistically significant. In other words, the data from the present study varies more than would be expected based on the study by Lee et. al [17].

Having found evidence that the variance in the two samples varies significantly, a type of modified t-test that is often referred to as Welch's t-test was used to examine the difference in the means. For Welch's t-test, the so called t statistic is calculated using

$$t = \frac{\overline{Y}_1 - \overline{Y}_2}{\sqrt{\frac{S_1^2}{N_1} + \frac{S_2^2}{N_2}}} \tag{7.12}$$

where t is the t statistic, and N_1 and N_2 are the number of elements in sample one and sample two respectively. Welch's t-test also requires the degrees of freedom to be calculated. This can be approximated through the use of the Welch-Satterwaite equation

$$\nu \approx \frac{\left(\frac{S_1^2}{N_1} + \frac{S_2^2}{N_2}\right)^2}{\frac{S_1^4}{\nu_1 N_1^2} + \frac{S_2^4}{\nu_2 N_2^2}} \tag{7.13}$$

where ν is the degrees of freedom for the t-distribution and ν_1 and ν_2 are the degrees of freedom for the samples one and two respectively. The values of t and ν were calculated to be 1.78 and 23.96 respectively. This results in a p-value of 0.878, which indicates that there is almost no evidence to suggest that there is a meaningful difference in the mean values.

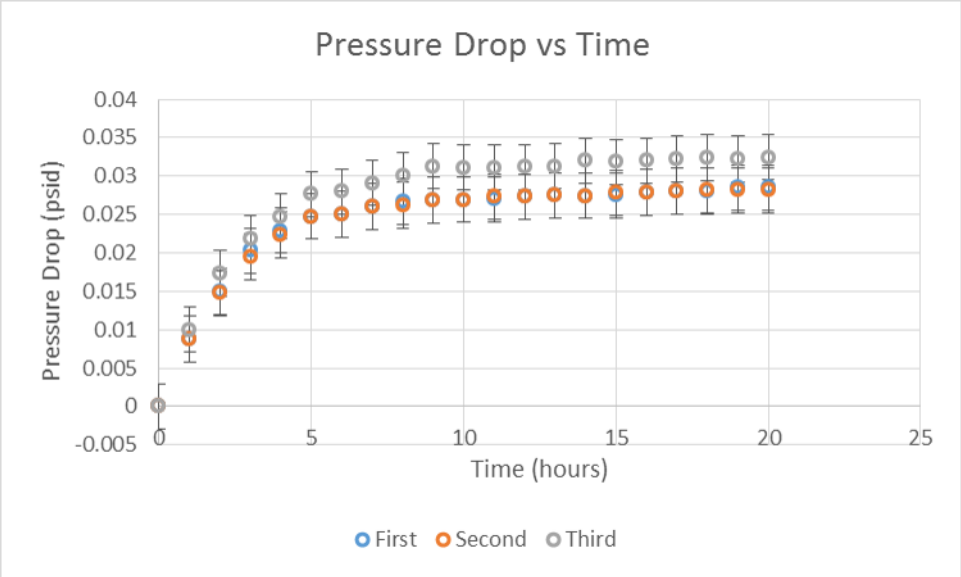

Figure 7.1: Head loss over time results obtained by Abdulsattar (Recreated from Head Loss Through Fibrous Debris Bed with Different Types of Perforated Strainers [8]).

7.3 Head Loss

The results of the head loss were compared to previous head loss results obtained by Abdulsattar as can be seen in Figure 7.1 [8]. More specifically, pressure drop in the present study was compared to pressure drop results obtained using the same strainer based on the STP sump strainer, at a flow rate of 0.122 in/s (0.311 cm/s). Because the previous pressure drop study was conducted with a significantly higher initial concentration of NUKON, away must first be found to correlate the present results to the previous. Developing such a correlation is based on the assumption that the pressure drop at the end of a test during the present study will be approximately the same as the pressure drop during a test in the previous study at some intermediate time, t_f.

The rate of change in the mass of the debris in the water tank can be expressed as

$$V_T \frac{d\,C(t)}{dt} = \dot{m}_{in}(t) - \dot{m}_{out}(t) \tag{7.14}$$

where V_T is the volume of water in the tank, $C(t)$ is the time dependant concentration of debris in the tank (measured in mass per volume), t is time, $\dot{m}_{in}(t)$ is the time dependant mass flow rate of debris into the tank, and $\dot{m}_{out}(t)$ is the time dependant mass flow rate of debris out of the tank. Given that all debris exiting the tank are trapped by the strainer or in the filter bag, $\dot{m}_{in}(t)$ can be assumed to be zero. Assuming the concentration of debris to be perfectly uniform, $\dot{m}_{out}(t)$ can be expressed as a function of time

$$\dot{m}_{out}(t) \;=\; U\; A\, C(t) \tag{7.15}$$

where U is the average flow velocity out of the tank, and A is the area of the outlet. Based ont the above definitions and assumptions, Equation 7.14 can be rewritten as

$$V_T \frac{d\, C(t)}{dt} \;=\; -U\; A\, C(t) \tag{7.16}$$

which is an ordinary differential equation with a solution in the form of

$$C(t) \;=\; C_o\; e^{\frac{-U\,A\,t}{V_T}} \tag{7.17}$$

where C_o is the initial concentration in the tank. Substituting Equation 7.17 into Equation 7.15 yields

$$\dot{m}_{out}(t) \;=\; U\; A\, C_o\; e^{\frac{-U\,A\,t}{V_T}} \tag{7.18}$$

The total mass of debris in the test section at any given time t_f is found by integrating Equation 7.18 as follows

$$\int_0^{t_f} U\; A\, C_o\; e^{\frac{-U\,A\,t}{V_T}}\, \mathrm{d}t. \tag{7.19}$$

which has a general solution of

$$m_{tot} \;=\; V_T\, C_o \left(1 \;-\; e^{\frac{-U A t_f}{V_T}}\right) \tag{7.20}$$

where m_{tot} is the total mass of debris in the test section.

When the mass of debris in the test section in the current study is equal to the mass of debris in the previous study then the equation

$$V_{T1}\, C_{o1} \left(1 \;-\; e^{\frac{-U_1 A_1 t_{f1}}{V_{T1}}}\right) \;=\; V_{T2}\, C_{o2} \left(1 \;-\; e^{\frac{-U_2 A_2 t_{f2}}{V_{T2}}}\right) \tag{7.21}$$

where the subscript 1 corresponds to the previous study and the subscript 2 corresponds to the present study. If the volumes, flow velocities, and areas are the same, then Equation 7.21 can be simplified and solved for t_{f1} resulting in

$$t_{f1} \;=\; -\,\frac{V_T}{U\,A} Ln \left[1 \;-\, \frac{C_{01}}{C_{02}} \left(1 \;-\; e^{\frac{-U_2 A_2 t_{f2}}{V_T}}\right)\right] \tag{7.22}$$

which yields a value of 13.82 minutes for T_{f1}. Interpolating Abdulsattar's results produces an average pressure drop of 0.002149 $\pm$ 0.000245 psid (14.8 $\pm$ 1.7 Pa). The avarage pressure drop in the present study was found to be 0.001935 $\pm$ 0.000616 psid (13.3 $\pm$ 4.2 Pa). Performing a t-test on the pressure drop results results in a P-value of 0.316, which indicates that the pressure drop results are in relatively good agreement.

7.4 Hypotheses and Further Work

7.4.1 Bypass

A number of different ideas were explored to try and explain the eccentricities noted above. First, it was noted that the previous tests with applied voltage were run at 77 $\pm$ 5.4°F (25 $\pm$ 3°C), whereas the present study was run at 69.8 $\pm$ 4.7°F (21 $\pm$ 2.6°C). A t-test reveals that this difference is statistically significant (with a P-value of 0.00047).

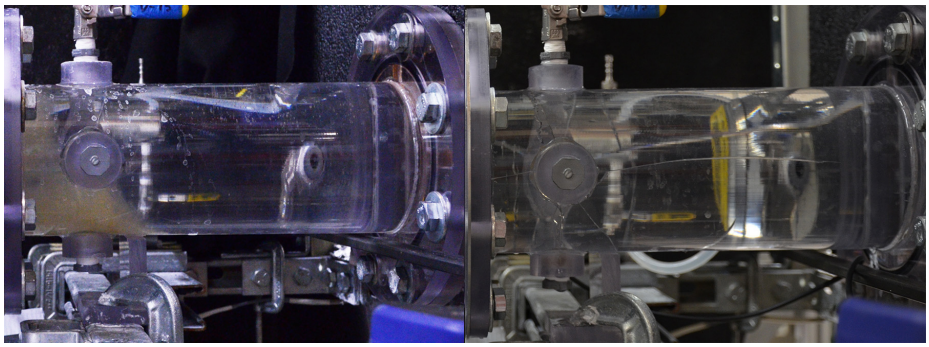

Figure 7.2: Crack formation in the test section (Section at the beginning of the present study is seen left and after cracks developed during the present study is seen right).

This difference is enough to cause the kinematic viscosity to be 8.9% lower in the present study. It is unclear though, in the literature, whether or not an 8.9% difference would have a significant impact on the bypass.

Second, repeated bolting and unbolting of the pipes that make up the test section have stressed them to the point that they have cracked and begun to leak (see Figure 7.2). The author had been assured that past experiments have successfully run despite such leaks. Because of this, no formal effort was made to measure and document the rate of leakage. Informal observations showed that, at their peak before being repaired, the water level in the tank dropped as much as 2" (5.08 cm), corresponding to 5 gal (18.9 L). This equates to a leakage rate of 2.39 gal/hr (9.05 L/hr), which corresponds to 10.3% of the flow rate through the loop. However, there is no way to tell how much this may have affected the results or even which tests had significant leakage. Concerns were also raised that a leak in the test section could compromise the electric field applied to the strainer.

Finally, Abdulsattar noted that, despite the manufacturer's guarantees that all NUKON mats have the same properties, the pressure drop through a NUKON debris bed can vary

depending on the mat from which the debris was prepared [8]. It is conceivable that the amount of debris bypass could similarly vary from mat to mat.

7.4.2 Pressure

Given the number of tests performed in the present study, two NUKON mats were used. It is possible, therefore, that this contributed to the difference between -1 V and the rest of the tests. However, this is unlikely to have been the only factor responsible. In his study of pressure drop, Adbulsattar found that pressure drop can vary by as much as 10.5% [8]. While the conditions in the present study were not examined in Abdulsattar's work, it is unreasonable to believe that a difference of 28.5% could be the result of different mats alone.

It was noted that the tests run at -1 V tended to be warmer than the tests run at the other voltages. An ANOVA found the P-value associated with this difference to be 0.081. Previous experiments have shown that higher temperatures result in lower pressure drop [30].

In addition to being run at higher temperatures, it was noted that three of the four tests run at -1 V were run during the first half of the present study when the cracks and leaks were at a minimum. It's possible that as the cracks worsened, the increased surface roughness increased the turbulence of the flow and altered the debris bed formation, resulting in the increased pressure drop seen in other experiments.

8. CONCLUSION

A horizontal flow loop was used to test the effect of applied voltage on the amount of fibrous NUKON debris bypass on a containment sump strainer. Previous work indicated that a voltage applied would have a significant impact on the bypass, however this work only included single data points and therefore carried no statistical weight. A battery of tests were run at voltages of -2, -1, -0.5, 0.5, and 1 V. The trend observed in the previous work was not observed, furthermore a single factor ANOVA revealed that the debris bypass does not vary with the strength of the applied voltage, neither does the pressure drop through the debris bed.

The bypass results of the present study show some abnormalities. Both the mean and standard deviation in the present study were higher than expected. The difference between the mean bypass value in the previous and present studies was found to have mild statistical significance at most. The unusually high variation in the results of the present study was found to be higher by a statistically significant amount.

Four explanations were offered as possible causes for these discrepancies. First, it was noted that the water temperature was significantly lower than the temperature recorded in previous studies. This would have resulted in an 8.9% difference in kinematic viscosity. Second, cracks formed over time in the test section. This may have resulted in a leakage rate equal to as much as 10.3% of the flow rate through the loop. However, rigorous documentation of the leakage was not made. Third, a leak in the test section could compromise the electric field used in the study. Finally, it has been noted in the past that the NUKON mats used in preparing the debris can have an impact on the results.

The pressure drop measurements showed good agreement with previous work, but tests run at -1 V showed abnormally low pressure loss. This difference could be the result of two

different NUKON mats being used, slightly higher operating temperatures, and variations in surface roughness. It is unlikely that any one of these could be labeled as the sole cause, but all three together could be responsible.

The results from the present study could be better understood if effect of kinematic viscosity on bypass was better characterized. Additional research could also be done to investigate the effect that the leak may have had. Furthermore, tests should be run to see if the bypass varies from one NUKON mat to another.

If additional research is conducted on the effects of voltage on bypass, there are some improvements that could be made. First, more rigorous control of the water temperature could be implemented. Second, all the piping should be repaired or replaced as needed to ensure that there is no leakage. Finally, the electric current from the voltage source could be measured and recorded as a means of verifying that the voltage is being applied as expected.

REFERENCES

1. Sparks, T. (2012). *Solid-liquid filtration: a user's guide to minimizing cost & environmental impact, maximizing quality & productivity. Trevor Sparks.* [Oxford] : Butterworth-Heinemann, [2012].

2. Perlmutter, B. A. (2015). *Solid-liquid filtration : practical guides in chemical engineering. Barry A. Perlmutter.* Oxford, UK ; Waltham, MA : Elsevier Ltd., [2015].

3. Sutherland, K. (2008). *Filters and filtration handbook. 5th ed.* Oxford : Elsevier, 2008.

4. M. R. Fard, "Assessment of Debris Accumulation on PWR Sump Performance," U.S. Nuclear Regulatory Commission, NUREG-0933, Rev.2, Main Report with Supplements 1-34, Washington, D.C., March 29, 2012.

5. Rao, D. V. (2002). *GSI-191 technical assessment.* Washington, DC : Division of Engineering Technology, Office of Nuclear Regulatory Research, U.S. Nuclear Regulatory Commission :, 2002.

6. Dale, C. B., Sadasivan, P., & Leteller, B. C. (2006). *Effects of insulation debris on throttle-valve flow performance: a subtask of GSI-191. principal investigators, C.B. Dale, P. Sadasivan, B.C. Letellier; prepared by P. Sadasivan [and others].* Washington, DC : Division of Fuel, Engineering, and Radiological Research, Office of Nuclear Regulatory Research, U.S. Nuclear Regulatory Commission, 2006.

7. Fu, T., & Fullerton, A. (2006). *Hydraulic transport of coating debris : a subtask of GSI-191. principal investigators, T. Fu and A. Fullerton ; prepared by A. Fullerton [and others].* Washington, DC : Division of Fuel, Engineering, and Radiological

Research, Office of Nuclear Regulatory Research, U.S. Nuclear Regulatory Commission, 2006.

8. Abdulsattar, S. S., & Hassan, Y. A. (2015). *Head Loss Through Fibrous Debris Bed with Different Types of Perforated Strainers. by Suhaeb Sabah Abdulsattar.* [College Station, Texas] : [Texas A & M University], [2015].

9. McMurry, J. (2006). *GSI-191 PWR sump screen blockage chemical effects tests : thermodynamic simulations. prepared by J. McMurry [and others].* Washington, DC : U.S. Nuclear Regulatory Commission, Office of Nuclear Regulatory Research, [2006].

10. Shaffer, C. J. (2005). *GSI-191 : experimental studies of loss-of-coolant-accident-generated debris accumulation and head loss with emphasis on the effects of calcium silicate insulation. prepared by C.J. Shaffer [and others].* Washington, DC : Division of Engineering Technology, Office of Nuclear Regulatory Research, U.S. Nuclear Regulatory Commission, 2005.

11. Ali, A., Williams, C., Blandford, E., & Howe, K. (2014). Filtration of particulates and pressure drop in fibrous media in resolution of GSI-191. *Transactions Of The American Nuclear Society, 111* (Transactions of the American Nuclear Society - 2014 ANS Winter Meeting and Nuclear Technology Expo), 967-970.

12. Hutten, *Handbook of Nonwoven Filter Media*, Butterworth-Heinemann, Oxford, UK, p.29 (2007).

13. S. Lee, R. Vaghetto, J. Lim, M. Kappes, Y. A. Hassan, "The Effect of Electric Potential on Fibrous Debris Bypass through a Containment Sump Strainer," Proceedings of the 16th International Topical Meeting on Nuclear Reactor Thermal Hydraulics (NURETH-16) NURETH15-13760

14. Kia, S., Fogler, H., & Reed, M. (1987). Effect of pH on colloidally induced fines migration. *Journal Of Colloid And Interface Science, 118*(1), 158-168. doi:10.1016/0021-9797(87)90444-9

15. Kolakowski, J. E., & Matijevi, E. (1979). Particle adhesion and removal in model systems. Part 1.Monodispersed chromium hydroxide on glass. *Journal Of The Chemical Society, Faraday Transactions 1: Physical Chemistry In Condensed Phases*, 7565. doi:10.1039/F19797500065

16. Khilar, K. C., & Fogler, H. S. (1998). *Migrations of fines in porous media. by Kartic C. Khilar and H. Scott Fogler*. Dordrecht ; Boston : Kluwer Academic Publishers, [1998].

17. Saya Lee, Yassin A. Hassan, Rodolfo Vaghetto, Suhaeb S. Abdulsattar, and Matthew Kappes, Water chemistry sensitivity on fibrous debris bypass through a containment sump strainer, *Proceedings of the 22nd international Conference on Nuclear Engineering (ICONE22)*, Prague, Czech Republic, July 7-11 (2014)

18. Lee, S., Vaghetto, R., Abdulsattar, S., Kappes, M., & Hassan, Y. (2014). Effects of pH and electrical conductivity on the quantity of fibrous debris bypass through a containment sump strainer. *Transactions Of The American Nuclear Society, 110*(2014 Annual Meeting - Transactions of the American Nuclear Society and Embedded Topical Meeting: Nuclear Fuels and Structural Materials for the Next Generation Nuclear Reactors, NSFM 2014), 645-648.

19. Lee, S., Vaghetto, R., & Hassan, Y. (2013). Measurement of water chemistry sensitivity on NUKON fibrous debris penetration through a sump strainer. *Transactions Of The American Nuclear Society, 109*(PART 2), 1935-1938.

20. STP Pilot Submittal and Request for Exemption for a Risk-Informed Approach to Resolve Generic Safety Issue (GSI)-191, NOC-AE-13002954, Docket Nos. STN 50-498 and STN 50-499, South Texas Project (2013)

21. J. C. Butler, ZOI Fibrous Debris Preparation: Processing, Storage, and Handling, NEI, Rev. 1 (2012).

22. W.W. Grainger Inc., Grainger Catalog, Catalog 405, Multifunction Timedelay, Dayton Model# 1EJE9, Global Company, 2014.

23. Shenzhen Korad Technology. (2011). *KA3000/6000-Series User Manual*. Retrieved from http://koradtechnology.com/en/cp-3.html

24. Honeywell International Inc., Ultra Precision Wet/Wet Differential Pressure Transducer, Model # TJE, May 2008.

25. Krohne. (2014). *Optifulx 1000 Handbook*. Duisberg: Author.

26. Keysight Technono (2014). *Keysight 34970A Data Acquisition/Switch Unit Family: Technical Overview*. Santa Rosa: Author

27. Nikon Corperation. (2010). *Digital Camera D7000 User's Guide*. Tokyo: Author

28. Mettler Toledo (2012). *SevenCompact^{TM} pH/Ion Meter S220: Operating Inscturctions*. Columbus, OH: Author

29. Eutech Instruments (2010). *Multi-parameter Testr 35 series*. Vernon Hills, IL: Author

30. Enderlin, C. .. (2007). *Experimental measurements of pressure drop across sump screen debris beds in support of generic safety issue 191. prepared by C.W. Enderlin [and others]*. Washington, DC : U.S. Nuclear Regulatory Commission, Office

of Nuclear Reactor Regulation, Division of Risk Assessment and Special Projects, 2007.